Renewable and Sustainable Energy Reviews 22 (2013) 81–91

Contents lists available at SciVerse ScienceDirect

Renewable and Sustainable Energy Reviews

journal homepage: www.elsevier.com/locate/rser

Considerable parameters of using PV cells for solar-powered aircrafts

Farivar Fazelpour, Majid Vafaeipour*, Omid Rahbari, Reza Shirmohammadi

Department of Energy Systems Engineering, Islamic Azad University-South Tehran Branch, Tehran, Iran

A R T I C L E I N F O

Article history:
Received 2 August 2012
Received in revised form
4 January 2013
Accepted 14 January 2013
Available online 28 February 2013

Keywords:
Solar powered aircraft
Photovoltaic cell
Efficiency
MPPT
UAV

A B S T R A C T

Parameters such as heat transfer, arrangement type, covering and deviation from tilt angle of PV cells located on the wings of a solar-powered aircraft impact on the efficiency, power, flight duration and costs of the solar flyer. The objective of this paper is to represent these parameters and their influence on the efficiency and power to be considered before constructing. Related equations for design process and selecting PV cells are represented and discussed. Solar irradiance is not monotonic during the flight. Hence, components and algorithms for designing a MPPT (Maximum Power Point Tracker) device from perspective of being utilized in solar-powered aircrafts are investigated. Furthermore, heat transfer on the cells of the wings and its influence on the efficiency is discussed which can help to make up the power reduction caused by covering and deviation from tilt angle of the cells.

Contents

* Corresponding author. Tel.: +989379111540.
E-mail address: st_m_vafaeipour@azad.ac.ir (M. Vafaeipour).

1364-0321/$ - see front matter
http://dx.doi.org/10.1016/j.rser.2013.01.016

Nomenclature

V_{OC}	open-circuit voltage (V)
I_{SC}	short-circuit current (A)
$I_{L(G_0)}$	current at constant sun intensity (A)
$I_{l(G)}$	current at various irradiance levels (A)
I_S	reverse saturation current (A)
Q	electric charge (c)
K	Boltzmann constant (J/K_0)
k_T	mounting coefficient
G_0	sun intensity (kW/m^2)
G	irradiance (kW/m^2)
G_{poa}	instantaneous plane-of-array irradiance
I_{max}	maximum irradiance in a day
A_C	irradiance level (W/m^2)
A_{sc}	surface of solar cell (m^2)
T_C	cell temperature
T	absolute temperature
T_a	ambient temperature
T_b	temperature on PV back surface
ΔT	temperature difference
Y	width (m)
η_r	standard reference efficiency
η_{wthr}	weather clearness coefficient
η_{camber}	cambered shape coefficient
η_{sc}	efficiency solar cell
η_{mpp}	efficiency of the maximum power point tracker
FF	fill factor
$E_{day\ density}$	daily solar energy density
$E_{elec\ total}$	electric energy (W)
NOCT	normal Operation Cell Temperature
h	convection heat transfer coefficient (W/m^2 K)
h_{free}	free convection heat transfer coefficient (W/m^2 K)
h_{force}	force convection heat transfer coefficient (W/m^2 K)
K	conduction heat transfer coefficient (W/m^2 K)
L	length of the surface (m)
V	wind speed (m/s)
R_e	Reynolds number
nu	Nusselt number
q''_{cond}	conductive heat transfer
q''_{rad}	radiation heat transfer
$q''_{conv.}$	convection heat transfer
α	absorption coefficient
τ	transmission coefficient
T_{day}	day length (h)
θ	angle
k_{mppt}	mass to power ratio of the MPPT (kg/W)
$P_{loss_{Vsense}}$	voltage sensing power loss
$P_{loss_{Isense}}$	current sensing power loss
$P_{conduct}$	conduction loss
P_{eq-cap}	diode equivalent capacitance power loss
P_{gate}	gate power loss
$P_{ind_{res}}$	inductors power loss
k_{mppt}	mass to power ratio of the MPPT
m_{mppt}	mass of the MPPT

1. Introduction

1.1. Employing solar energy for flight

Solar cells or photovoltaic (PV) cells, as devices of converting solar energy into electricity, were produced in the late 1950s, and throughout the 1960s were exclusively used to provide electrical power for earth-orbiting satellites [1]. Gradually as a result of technology advances, serious environmental awareness, growing electricity demands and limited fossil resources sun harnessing became a chief role player in the humanities search for clean energy. Today, the industry's production of PV modules is growing at approximately 25 percent annually [1]. Applying solar energy for flight is one of the most promising utilizations of renewables which has attracted many researches nowadays. Solar-powered aircrafts can be employed for high altitude communication platforms, border surveillance, forest fire fighting and power line inception. They can also be used as an alternative to supersede scientific, environmental and communication satellites or to be used for monitoring crops as well as civil applications.

Table 1
Efficiency and technology advances of solar cells [2].

Module	Technology	Efficiency (%)
Sun power 315	Mono-Si, special junction (sp. j.)	19.3
Sanyo HIP-205BAE	CZ-Si, HIT, sp. j.	17.4
BP7190	CZ-Si, sp. j.	15.1
Kyocera KC200GHT-2	MC-Si, standard junction (std. j.)	14.2
Solar world SW 185	CZ-Si, std. j.	14.2
BP SX3200	MC-Si, std. j.	14.2
Suntech STP 260 S-24 V/b	MC or CZ-Si, std. j.	13.4
Solar world SW 225	MC-Si, std. j.	13.4
Evergreen solar ES 195	String-ribbon-Si std. j.	13.1
Wurth solar WS11007/80	CIGS	11
First solar FS-275	CdTe	10.4
Sharp NA-901-WP	a-Si/nc-Si	8.5
GSE Solar GSE120-W	CIGS	8.1
Mitsubishi heavy MA100	a-Si, single junction	6.3
Uni-solar PVL136	a-Si, triple junction	6.3
Kaneka T-SC(EC)-120	a-Si single junction	6.3
Schott solar ASI-TM86	a-Si/a-Si same bandgap tandem	5.9
EPV EPV-42	a-Si/a-Si same bandgap tandem	5.3

Obtaining sufficient flight power is hand in hand with selecting PV cells in an appropriate way and considering weight and efficiency is a key to a high endurance flight in solar-powered aircrafts. Different technologies and materials are employed to gain higher efficiencies as well as cost-effectiveness of solar cells up to now, which is evident in Table 1 provided by the National Energy Renewable Laboratory (NERL), USA, using the highest PV modules efficiency data existed on manufacturers' web site in April 2008 [2]. But it is still essential to improve PV cells and investigate higher efficiency conditions to employ them more widely in higher availability and performance.

1.2. Environmental and meteorological effective factors on the efficiency

Efficiency of a solar cell depends on many environmental features and weather parameters such as humidity, wind speed, dust, temperature, shading, tilt angle, azimuth plane angle, sun intensity, etc. Throughout the literature, influence of these parameters on the efficiency has been the subjects of a number of investigations. The sun intensity is considered as an obvious influential factor on efficiency. In summer and spring, due to more intensity of the sun, a solar cell is more able to kick lose its electrons from the parent atoms, and it is also because of this factor that it performs better in the sunnier areas. It is showed that humidity causes irradiance degradation, and lower efficiency is resulted in its presence [3–5]. Dust caused efficiency reduction

of 1% with a peak of 4.7% in a 2-month period [6] and 32% reduction in a 8-month time [7] in USA and Saudi Arabia respectively. Wind for causing convection heat transfer, as well as lowering relative humidity and temperature, is a pleasant factor to gain higher efficiency. This is effective especially when the cells are arrayed on a speeding object such as the wings of a solar-powered aircraft. But on the other hand, dust lifting by the wind leads to shading and occurrence of efficiency reduction [8].

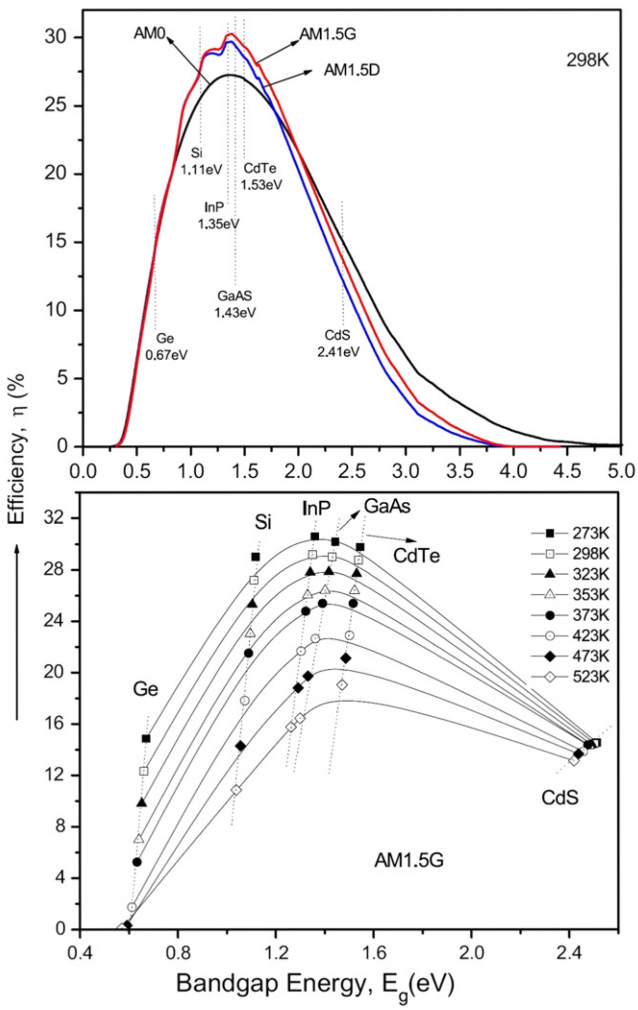


Fig. 1. Dependency of the band gap, temperature and efficiency [18].

As a characteristic of semiconductors, solar cells are sensitive to temperature. A part of photo-voltaic energy which is not converted into electricity will appear in the heat form of energy in solar cells and elevates temperature of the cell. In the earlier studies and contrary to popular belief, it is showed that the efficiency of solar cells degrades with the increasing temperature [9–15]. The reason is that high temperature increases the conductivity of semiconductors. Properties of a semiconductor define its suitability for being used in PV cells. One of these properties is the so-called band gap, which is the energy gap an electron must cross in order to be promoted from the valence band to the conduction band. Increase in temperature reduces the band gap of a semiconductor [16,17]. Fig. 1 illustrates the dependency of band gap, temperature and efficiency with respect to the content elements of solar cells in standard test conditions (STC) [18].

2. The characteristics of conversion efficiency, electricity analysis

Short-circuit current I_{sc} and the open-circuit voltage V_{oc} are two important parameters of the nonlinear IV curve for a PV module. In Fig. 2, the point at which a curve intersects the vertical axis is known as the short circuit condition, and it defines how the cell operates if a wire is connected between its terminals, shorting it out. The current flow here is known as the short-circuit current, I_{sc}. For an ideal solar cell at most moderate resistive loss mechanisms, the short-circuit current and the light-generated current are identical. Therefore, the short-circuit current is the largest current which may be drawn from the solar cell. The point at which a curve intersects the horizontal axis is known as the open circuit condition. The open-circuit voltage, V_{oc}, is the maximum voltage available from a solar cell, and this occurs at zero current. The open-circuit voltage corresponds to the amount of forward bias on the solar cell due to the bias of the solar cell junction with the light-generated current. V_{oc} depends on the saturation current of the solar cell and the light generated current. Open-circuit voltage is then a measure of the amount of recombination in the device [19]. I_{sc} and V_{oc} change with the incident solar irradiance and with the ambient air temperature T_a. The short-circuit current is approximately proportional to the incident solar irradiance and the open-circuit voltage increases just a little when the solar irradiance increases. On the other hand, it is important to note that V_{oc} decreases with increasing module temperature which leads to a noticeable decrease in the available maximum electrical power, in spite of a small increase of the short-circuit current *Isc* [20,21]. As discussed, effective

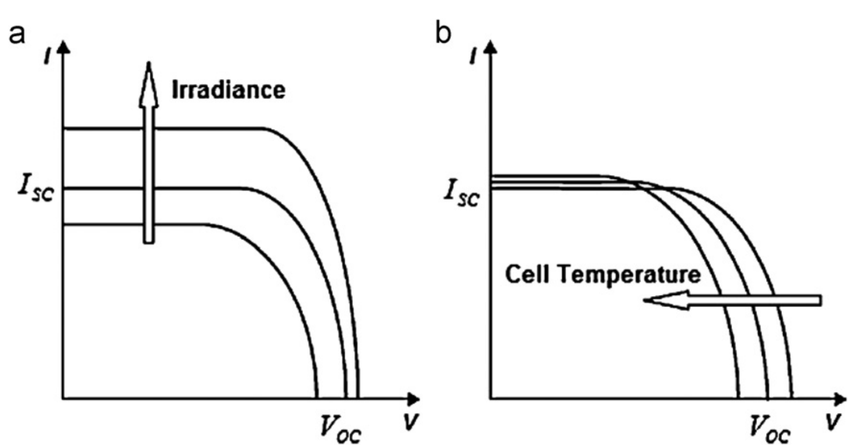


Fig. 2. *I–V* curve for a PV cell.

parameters on a PV cell have an interplay and depend on the conditions. It is therefore possible that a single solar cell's performance varies widely depending on its location. So, the nominal power of a solar cell is generally expressed in Wattpeak (Wp), which represents its efficiency under laboratory conditions (standard test condition (STC)). These conditions are set at a temperature of 25 °C, light travel distance of 1.5 air mass and a light intensity of 1 kW/m^2. But this theoretical limit is almost never reached in an outdoor online device. Current and voltage play an important role in the *I*–*V* curve and therefore in maximum power point tracking of solar cells. The *I*–*V* characteristic equation (diode equation) is given below where *k* is the Boltzmann constant [22].

$$I = I_L - I_s\left(e^{\frac{qv}{kT}} - 1\right) \tag{1}$$

In the above equation, $q = 1.6 \times 10^{-19}$ colon, $k = 1.38 \times 10^{-3}$ (J/K$_0$) and I_s is the reverse saturation current which depends on the temperature and cell current at various irradiance levels can be calculated by the following equation [22].

$$I_L(G) = \left(\frac{G}{G_0}\right) I_L(G_0) \tag{2}$$

where G_0 will be the sun intensity equal to 1 kW/m^2, AM 1.5 and $I_L(G_0)$ is the cell current at G_0. To calculate the open circuit voltage which is logarithmically depended on cell illumination Eq. (3) can be employed [23]:

$$V_{oc} = \frac{kT}{q}\ln\left(\frac{I_l}{I_0} + 1\right) \approx \frac{kT}{q}\ln\left(\frac{I_L}{I_0}\right) \tag{3}$$

where *k*, *T* and *q* are the Boltzmann constant, absolute temperature and electronic charge respectively. Using the following equation maximum power extracted from a PV cell can be found where fill factor (FF) shows the quality of the solar cell [24].

$$P_{max} = (I_{max})(V_{max}) = (\mathrm{FF}) \cdot (I_{sc}) \cdot (V_{oc}) \tag{4}$$

And the conversion efficiency of a solar cell is formulated as follows in Eq. (5).

$$\eta = \frac{I_{sc-max} \cdot V_{oc-max}}{A_c(irradiance\ level)} \tag{5}$$

According to the mentioned equation to maximize the efficiency of a solar cell, the defined I_{sc}, V_{oc} and FF should be boosted up.

3. Maximum power point tracker (MPPT)

3.1. An introduction on MPPT and battery

The generated power during the flight of a solar-powered aircraft widely depends on load current, temperature, date, the time of day, the inclination of the cells with respect to the sun and the level of clouding [25,26]. Due to unpredictable nature of solar energy, the irradiance and as a result the output power which is being drawn from the cells on the wings are not monotonic during the flight. In addition, due to the small area of the array to be built on the wings, the output voltage is relatively low. On the other hand, as it is showed in Fig. 3, different energy consuming electric devices should be fed by battery and solar cells during the flight such as servos, motor, GPS, RC receiver, radio modem, etc. to transfer energy and data. To satisfy the demands and to overcome the unpredictability and uncertainties of solar energy, an electronic circuit which is called MPPT (Maximum Power Point Tracker) is required. MPPT keeps the current and voltage working for a maximum power regardless of changes in atmospheric conditions or load and optimizes the utilization of PV cells. Also, using MPPT as a supplement of the flight system lets more excess power charge the battery. So the power supply system is consisted of PV cells, MPPT and the battery. As it can be seen in Fig. 4, the MPPT directly connects to the battery and has the same voltage. The power requirement for climbing from launch is 12 times that of the power required for level flight. To size an array for this power output would be impracticable as the array would be designed for a peak demand that lasts a very small percentage of the total flight time. Secondly, when the model is cruising in good light conditions and/or at low throttle settings the array will be forced away from its maximum power point. By placing a battery between the MPPT and the motor controller both these problems can be addressed. The battery can supply the necessary current for a short burst of power required for the climb from launch, and

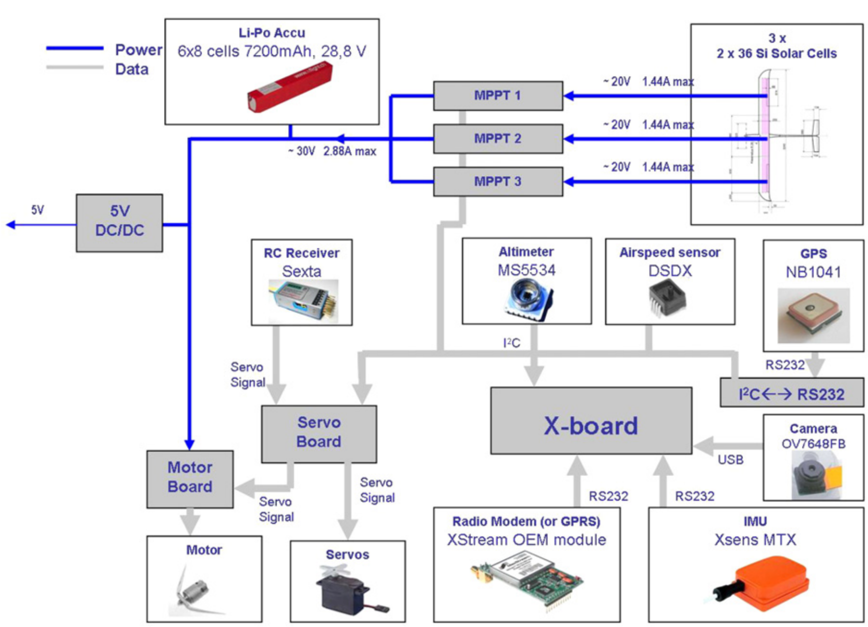


Fig. 3. Schematic of electric devices in a solar-powered aircraft [53].

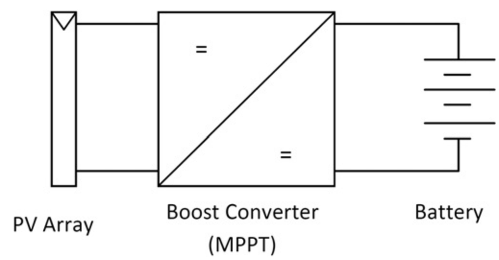


Fig. 4. Power supply schematic.

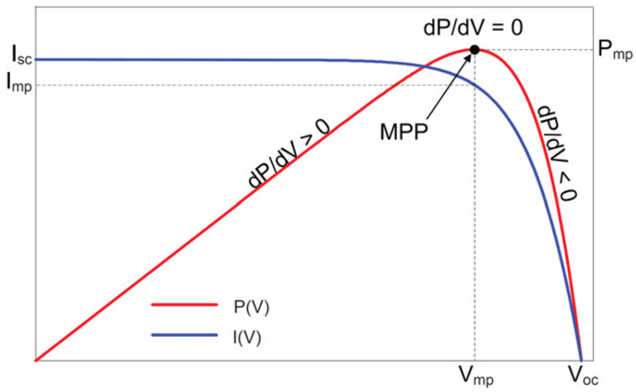


Fig. 5. Different positions on the power characteristic of a PV module.

when the power produced by the array is greater than the demand of the power train then this power can be stored by charging the battery (this is limited by the capacity of the battery). This will maximize the harvest of available solar radiation. Lithium-Polymer batteries are cheap, and readily available in a range of voltages and capacities. They are used extensively in model aircrafts and have higher discharge rates than other technologies which come at the expense of energy density. The typical energy density of Lithium-Polymer batteries designed for radio control aircrafts is in the vicinity of 140 Wh/kg [27].

A well-designed MPPT can be mentioned as an important key to a high endurance flight. The specifications for the circuit design must be done according to the target of the flight and electrical conditions at which the aircraft will operate. Designing of the MPPT circuit can include the following features [28]:

- Monitoring the input and output voltage and current as well as board temperature.
- Capability to report these measurements over the network.
- Continuous circuit adjustments to achieve maximum efficiency.
- Ability to shut down or throttle gracefully to prevent component failure.
- Physical switches to isolate the MPPT from the solar array and battery array in an emergency situation.

Considering Fig. 5 which illustrates *P–V* and *I–V* curves [29], the maximum produced power by PV cell is where *P* has its most value and this occurs at the knee of the curve. The fundamental idea behind using MPPT is to keep the power as close to this maximum power point using maximum power point tracking algorithms. Hence, a processor is being used to implement the desired tracking algorithm after measuring voltage and current coming from the cells by means of measurement. The power can be calculated and the output voltage of the solar array can be altered to maximize power by a micro-controller which regulates the gain of a DC–DC converter. The typical operating voltage of brushless DC motors for radio controlled aircrafts is approximately 12 V. For this reason, the MPPT designed for such projects adopts a boost converter topology [27].

3.2. *Components of MPPT*

From the latest explained part, micro-controllers, DC–DC converters and means to measure voltage and current are the main components of the circuit for maximum power point tracking. Hence, smart choice of these components plays an important role for an efficient flight.

3.2.1. *Micro-controllers*

Micro-controllers are consisted of resistors and capacitors. They control the gain of the DC–DC converter as well as the implementation of the MPPT algorithms. For easy removal of the program microcontrollers, a zero insertion socket can be used in the circuit. Using nanoWatt technologies, parameters such as small size, low power consumption and the output numbers must be considered while selecting controllers. In addition, the number of outputs should be adequate to support the required connections of motor speed controller and MPPT of the solar Unmanned Aerial Vehicle (UAV).

3.2.2. *Means of measuring voltage and current*

For measuring voltage, a device containing two resistors can be used. The power loss due to voltage sensing of these resistors is relatively small comparing with other power losses [26]. Voltage can be measured and converted into a digital value directly by the microcontroller's built-in analog to digital converters [28]. For measuring the current, the output current of the converter can be measured by using a shunt resistor. The voltage drop across a very low ohmic shunt resistor gets amplified by a current sense amplifier and feeds to one of the analog in pins of the microprocessor. Due to noise across the current sense resistor, adding a differential filter to the inputs greatly improves the quality of the output of the amplifier [27]. Current also can be measured using current sensing integrated circuits. These ICs measure the current and convert it to an analog voltage that is easily readable by microcontroller. It is also possible to measure the current using a resistor network, but this method is not as precise as measuring it directly [28].

3.2.3. *DC–DC converters*

DC–DC converters convert one DC voltage level to another level. These converters store the input energy in magnetic or electrical storing elements (inductor, capacitors) temporarily to release it at a different voltage. For controlling these components, an external signal, which is depended on the programmed algorithm, drives a transistor switch which opens and closes periodically [30]. As it can be seen in Fig. 6a, when the switch is closed, the diode in the circuit gets reverse bias and the supplied current by the source stores energy in a magnetic field (inductor). Opening the switch (see Fig. 6b) makes the diode in the circuit to get forward bias, the current redirects to the load and the stored energy in the inductor releases. The duty cycle represents the fraction of time the switch is on divided by the period of the waveform applied to the gate of the switch. If the duty cycle is increased, the output voltage increases and conversely if the duty cycle is decreased, the output voltage decreases [31]. Selecting capacitors and inductors should be done based on the required inductance and capacitance values, the saturation current and the working temperature range. Schottky diodes are the most common diodes used in DC–DC converters operating at very low

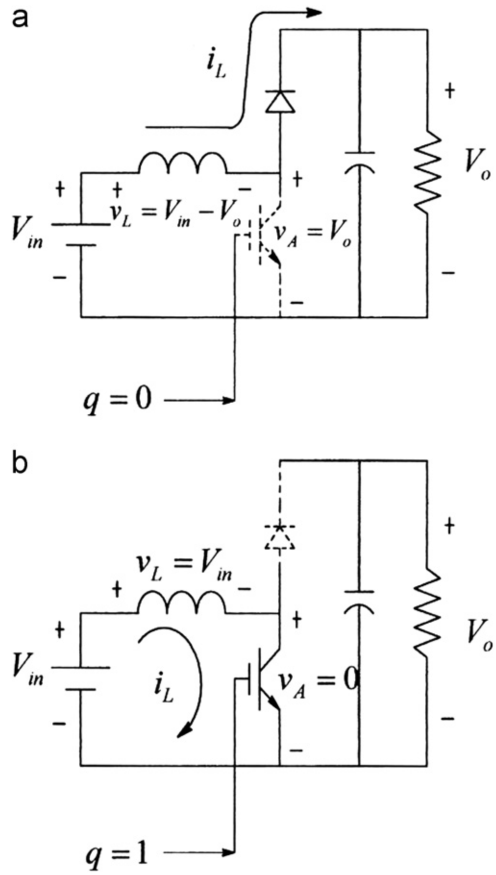


Fig. 6. (a) Boost DC–DC converter—opened switch status. (b) Boost DC–DC converter—closed switch status.

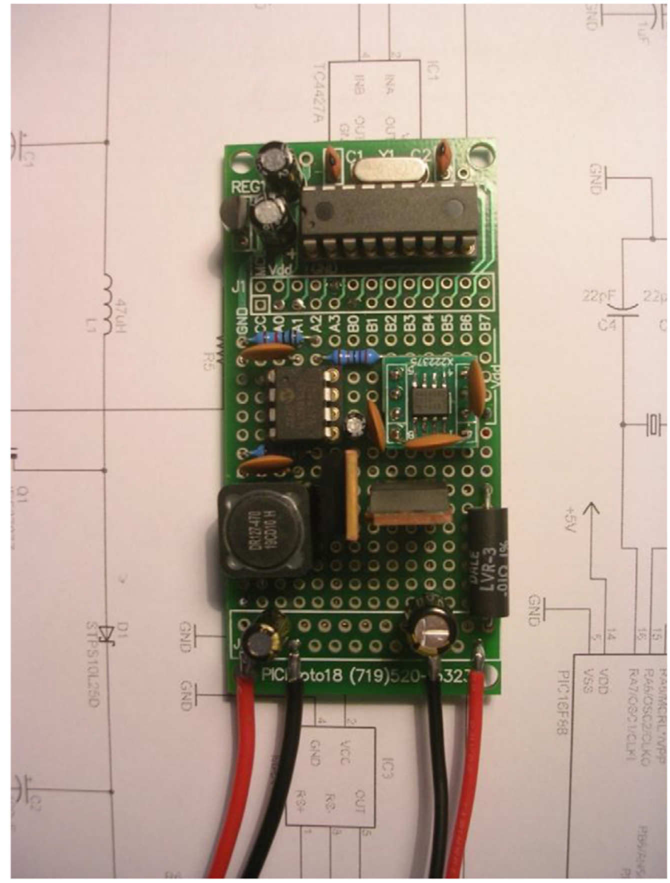


Fig. 7. A lightweight and efficient MPPT device [27].

voltage and high switching frequencies. Schottky diodes have a forward voltage drop of between 0.3 and 0.5V compared to approximately a volt for conventional p–n junction diodes which reduces conduction losses. Schottky diodes also switch extremely fast leading to negligible switching losses [31].

3.3. Weight and cost of MPPT

In designing MPPT for a solar-powered aircraft, size, weight, the flight objective and costs are the other citable parameters that should be considered according to the expected duties. A lightweight and efficient MPPT device for a solar-powered aircraft is shown in Fig. 7 and Fig. 8 illustrates the schematic of a Lithium-Ion battery, cells and MPPTs for a solar-powered aircraft with 3 parted arrayed cells on the wing structure. Table 2 presents the costs, models and the quantity of the circuit components for maximum power point tracking in a solar-powered UAV [27].

Weight of the MPPT device as an effective parameter on the total weight of a solar-powered aircraft can be calculated using the following equation where k_{mppt} is the mass to power ratio of the MPPT (kg/W) [32].

$$m_{mppt} = k_{mppt} P_{maxpv} \tag{6}$$

3.4. MPPT algorithms

The MPPT control algorithm is usually applied in the DC–DC converter, which is normally used as the MPPT circuit. Suggested algorithms for MPPT systems vary in different points of view as follows [33]:

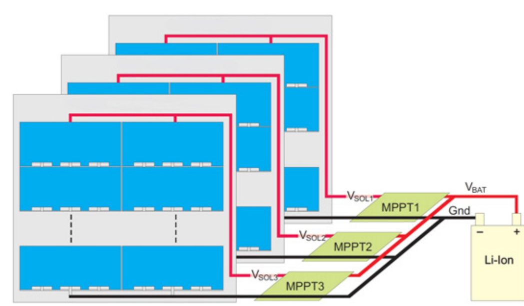


Fig. 8. Schematic of the solar generator [53].

Table 2
Costs, models and the quantity of circuit components [27].

Component	Quantity	Price
Microcontroller-PIC16F88	1	5.40
Schottky diode-STPS10L25D	1	2.39
Inductor-DR127-470-R	1	2.88
Capacitors	1	5.50
Current Sense Amp-Max4080	1	3.95
Resistors	4	0.80
5 V regulator	1	0.75
PICProto 18	1	9.95
MOSFET-IRF3707Z	1	2.73
MOSFET Driver-TC4427A	1	1.96
Crystal-20 MHz	1	0.58
Total	1	36.89

Accuracy: demonstrates the ability of the algorithm to reach to the actual maximum power point.

Speed: indicates how fast an algorithm can reach a stable point.

Power consumption (efficiency): introduces how much power the algorithm consumes considering the transferred power through the circuit (the algorithm and the MPPT circuit are both effective with regard to the efficiency).

Complexity and cost are other features of MPPT algorithm which depend on the expected activities of the circuit as well as the duration and objective of the flight. The costs and complexity are logically higher for a MPPT which reports the measurements on a network, utilizes adaptive duty cycle techniques, is armed with emergency shutdown option and adjusts the desired tracking more continuously. Also, if the algorithm is complicated, more engineers are needed to be employed for designing, programming and implementation to achieve desired results. Furthermore, a complicated algorithm needs a capable processor for calculating, which affects the total cost of the system. Although different MPPT algorithms are programmed, designed and implemented till now but optimizing these algorithms or presenting new algorithms and methods are still the interested fields of many researchers. Hill climbing methods [34], incremental conductance [33,35,36], P&O (Perturb and Observe), dp-P&O [37–39], fully analog algorithms, and advanced digital algorithms using artificial intelligence such as neural networks or fuzzy logic algorithms [25,33,40–42] are some of the popular algorithms which can be employed in the MPPT circuit of a solar-powered aircraft. P&O algorithms are of the so-called hill climbing methods. In these algorithms, the current and voltage are measured on the output of each DC–DC converter and the calculated power once compared with the previous value allows changing the gain into the correct direction. Due to their simplicity, low computational demand and accuracy, P&O algorithms are one of the most popular MPPT algorithms especially when optimizations are done [43]. Many of more complex algorithms rely on frequent tuning of parameters, whereas P&O is highly adaptive and works with no knowledge of the hardware on which it runs [33]. Conventional P&O algorithms suffer from some limitations. In steady state operation, they have oscillation around MPP and their response speed is lower than more advanced algorithms. In addition, they are not efficient under rapidly changing atmospheric conditions [44,45]. To overcome these limitations, efforts are done and optimized P&O algorithms are obtained using an additional measurement of the solar array's power in the middle of the MPPT sampling. These algorithms work based on the fact that in case of the *V–P* characteristic, on the left of the MPP the variation of the power against voltage $dP/dV>0$, while at the right, $dP/dV<0$ (Fig. 5). If the operating voltage of the PV array is perturbed in a given direction and $dP/dV>0$, it is known that the perturbation moved the array's operating point toward the MPP. The P&O algorithm would then continue to perturb the PV array voltage in the same direction. If $dP/dV<0$, then the change in operating point moved the PV array away from the MPP, and the P&O algorithm reverses the direction of the perturbation [46]. Figs. 9 and 10 illustrate the flow charts for P&O and dP-P&O algorithms.

In addition to the mentioned algorithms, Fuzzy Logic Control (FLC) algorithms are another citable type of algorithms which can be employed for MPPT systems. FLC systems are fast in tracking MPP and have simple design and high performance. Furthermore, FLC algorithms are independent from knowing the exact model of the system. It is showed that FLCs present faster response than conventional P&O techniques but their disadvantage is that they gain more energy than the other methods [25] and this gives limitations for employing them in solar-powered aircrafts. Conventional P&O method fails to track MPP when the atmospheric condition is rapidly changed but this method works well in the steady state condition (when the radiation and temperature conditions change slowly). Irradiation can change relatively quickly due to weather conditions, e.g. passing clouds and very fast changes corresponding to a variation of the rated power from 15% to 120% within 500 (ms) were reported (for small systems) [47]. Nevertheless, the probability of such fast irradiation changes is extremely low [46] and this makes P&O methods suitable for being employed in MPPT circuit of a solar-powered aircraft.

3.5. Efficiency of MPPT

Each introduced MPPT circuit components affects the total efficiency of the MPPT due to their related power losses. By adding all the related power losses, the total power loss will be as follows [26]:

$$P_{lost} = P_{loss_{Vsense}} P_{loss_{Isense}} + P_{conduct} + P_{eq-cap} + P_{gate} + P_{ind} P_{MOSFET_{res}} + P_{ind_{res}} \quad (7)$$

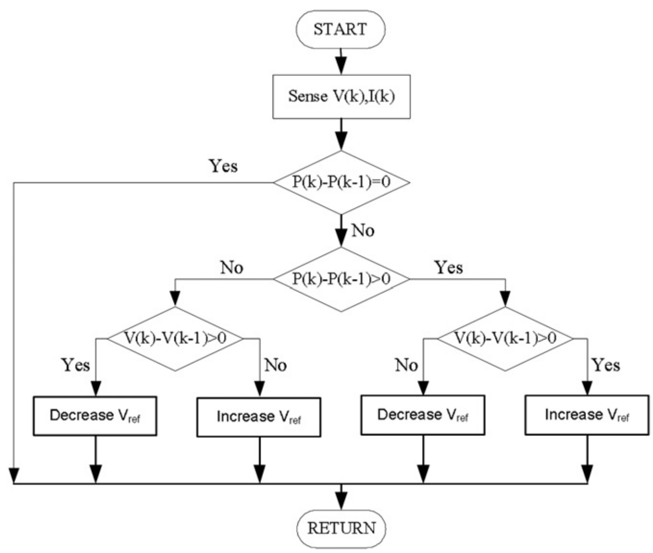


Fig. 9. Flowchart of P&O algorithm [46].

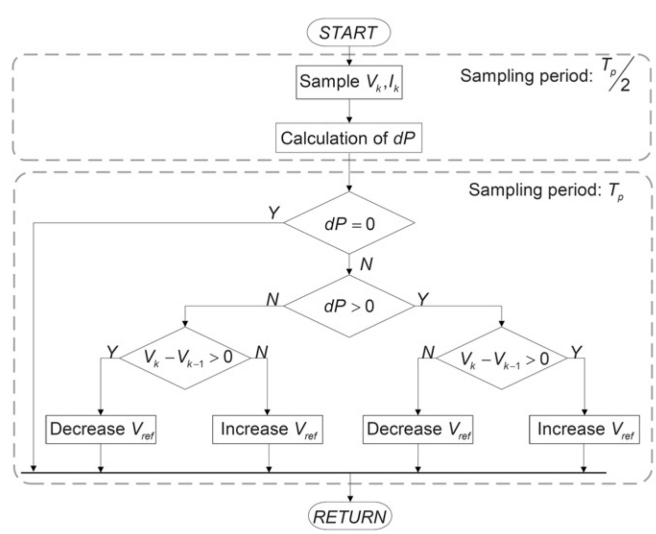


Fig. 10. Flowchart of dP-P&O algorithm [29].

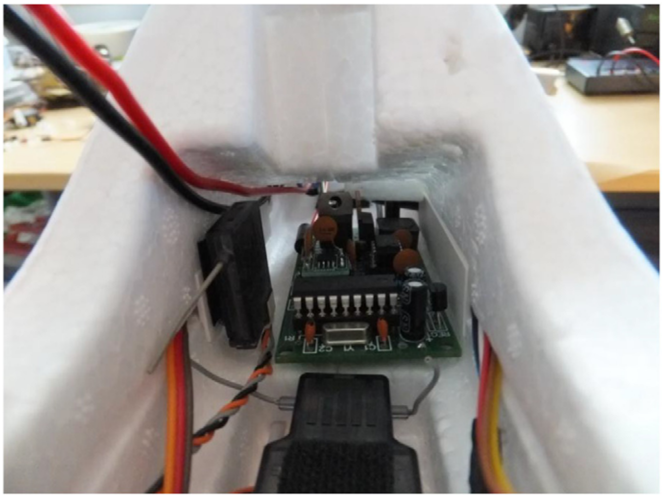


Fig. 11. MPPT installed in a fuselage [27].

where the parameters of the above equation to obtain total power loss are power loss due to voltage sensing ($P_{loss_{Vsense}}$), power loss due to current sensing ($P_{loss_{Isense}}$), conduction loss ($P_{conduct}$), diode equivalent capacitance power loss (P_{eq-cap}), charge of the gate power loss (P_{gate}), power loss in the MOSFET drivers ($P_{ind}P_{MOSFET_{res}}$) and the power loss in the inductors ($P_{ind_{res}}$).

At a maximum power P_{max} of W, the output will be

$$P_{out} = P_{max} - P_{lost} \tag{8}$$

And eventually, efficiency of MPPT can be calculated employing the above and the following equations.

$$\eta_{mppt} = \frac{P_{out}}{P_{max}} \tag{9}$$

It is specified that the efficiency of MPPT should be over 90% to be considered as a well-organized device [48].

3.6. Testing MPPT

After designing and constructing the MPPT must be tested in varying light conditions for observing the performance. Also, due to high frequency switching of the converter, interference between MPPT and the radio controller may occur. The noise caused by the converter can affect the radio control system and this may lead to the loss of an aircraft which does not have an autopilot system [27]. Hence, MPPT should house in the fuselage, Fig. 11 illustrates a completed MPPT installed in the fuselage of a solar-powered glider. Running MPPT at its maximum power and testing the performance of transmitter from a far desired distance ensures that there is no interference between MPPT and the control system for a safe flight.

4. Thermal analysis

Temperature of the cells is a function of several variables such as cell material, packing factor, thermal mass of PV modules, local wind speed and ambient weather conditions. The solar cell can not convert all of the photovoltaic energy directly into electricity. So as a result of the conversion loss and different kinds of heat transfer which will be discussed, PV cell is expected to operate at a temperature higher than the temperature of the ambient air. T_C is then dependent on the ambient temperature T_a and on the solar irradiance. The variation of cell temperature can be estimated with the ambient temperature via Eq. (10).

$$T_c = T_a + (NOCT - 20)\left(\frac{G}{800}\right) \tag{10}$$

where T_a is the ambient temperature, and NOCT is the normal operation cell temperature when operating at open circuit with the following conditions: ambient temperature of 20 °C, AM 1.5, irradiance of $G = 0.8$ kw/m^2 and wind speed less than 1 m/s [49]. Another formulation which can be used for steady state or slowly changing conditions to estimate T_c is [50]

$$T_c = T_a + k_T G_{poa} \tag{11}$$

where G_{poa} is the instantaneous plane-of-array irradiance and coefficient k_T strongly depends on the way that PV module is mounted (openrack, ventilated or unventilated roof mounting, etc.), wind speed (ν) and also on the module type [50]. Temperature in areas with low temperature can be directly estimated by the following equation too [51].

$$T_c = T_b + \Delta T\left(\frac{G}{G_0}\right), \quad 0 < \Delta T < 3\,^{\circ}\mathrm{C} \tag{12}$$

where T_b is the temperature on PV back surface and ΔT is a predetermined temperature difference. A known model which relates the cell temperature to efficiency is represented in Eq. (13) where η_r and T_0 have the standard reference test conditions quantities [20] which discussed before and in order to find T_c, Eq. (12) can be employed.

$$\eta = \eta_r\,[1 - \beta(T_c - T_0)] \tag{13}$$

In the above equation, β, which is dependent on the PV material, stands for the temperature coefficient of a PV module and is suggested equal to 0.0048 °C^{-1} for silicon [20]. From Eq. (13) it can be concluded that the efficiency decreases from its reference amount while temperature of the cell increases. Performing cooling tests, it is realized that the power degradation due to heat is 0.38% for every 1 °C over 25°, and for the temperature of the flight day, the loss can be calculated [52]. The array will be heated up to 65 °C in a day with average temperature of 35 °C when the cell is exposed to the sun, which results in loss of efficiency but the air flow cooling over a wing without a cover decreases the temperature to about 20 °C in less than 1 min at the speed of 50 Km/h. The cooling is much slower when the wings are covered and the temperature reaches 50 °C after 5 min for the same speed [53]. Speed of the aircraft as well as blowing wind cause cooling of the cells on the wings. The wind which blows from the opposite direction of flight has a more positive effect on power consumption. In addition to cooling of the cells, wind boosts up the lift force and less power is required during the flight. Cooling effect should be considered as an important parameter while designing the aircraft, selecting the cells as well as determination of the type of covering. This can result in buying less in amount or cheaper cells, and also higher flight endurance.

5. Energy balance

Investigation of the energy balance characteristics around the surface control which is the arranged PV cells on the airfoil of a solar-powered aircraft is presented in this section. In this case, 3 different kinds of thermal energy are flowing during the flight and cause different types of heat transfer (conduction, convection and radiation (see Fig. 12)). Thermal energy balance is given below:

$$q''_{conv.} = q''_{cond.} + q''_{rad.} \tag{14}$$

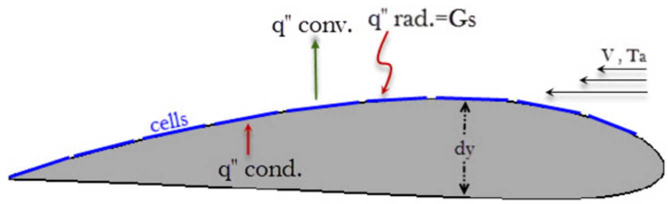


Fig. 12. Heat transfer scheme for the airfoil.

Eq. (15) explains the convection heat transfer as follows:

$$q''_{conv.} = h(T_c - T_a) \quad (15)$$

where h is the convection coefficient and is consisted of the sum of free and force convection coefficients:

$$h = h_{force} + h_{free} \quad (16)$$

The forced convection coefficient can be approximated as a function of wind speed using the Nusselt–Jurges correlation [54] which is given by

$$5.6212 + 3.9252(\,v_{wind}), \quad v_{wind} < 4.88 \ \ m/s$$

$$(3.29 v_{wind})^{0.78}, \quad 4.88 < v_{wind} < 30.48 \ \ m/s$$

And free convection coefficient for a flat plate as well as the airfoil of an aircraft (for the Reynolds numbers which will be discussed) can be calculated from the following equation:

$$h_{free} = 1.31 \sqrt[3]{T_c - T_a} \quad (17)$$

According to Eq. (18), convection coefficient is dependent on Nusselt number, and L is the length of the surface control in meter.

$$h = \frac{nu\, k_{air}}{L} \quad (18)$$

It is citable when Reynolds number is $R_e < 5 \times 10^5$, the Nusselt number and convection coefficient for the airfoil can be calculated almost the same as flow across a flat plate due to fully laminar flow over the surface of the airfoil [55]. So it should be noted that Eq. (16) can be used for the calculation of convection coefficient on the wings of a solar-powered UAV, because the Reynolds number is not that high in UAVs according to the cruise air speed during the flight.

Eq. (19) shows that conductive heat transfer is related to conduction coefficient (K), width (y), the temperature of the cell and the surface.

$$q''_{cond.} = \frac{-2K(T_c - T_s\,)}{y} \quad (19)$$

Considering the cover on the PV cells to form the airfoil shape of the wing structure as well as fastening and protecting the cells in flight, for a solar irradiance G, the part which crosses the cover is τG where τ is the transmittance of the cover system for diffuse radiation. The part absorbed by the photovoltaic cells is $\alpha\tau G$ and α is the absorption coefficient [20].

$$q''_{rad.} = \alpha\tau G \quad (20)$$

Various kinds of covering and mounting methods will result in different output powers at the same conditions. Table 3 represents some of these methods and the experimental loss of array efficiency in a solar powered-aircraft.

Table 3
Loss of array's efficiency for different covering methods [52].

Method	Loss (%)
Mylar cover	10
Transparent duct tape—full	5
Transparent duct tape—borders	1.5
Micro glass cover	20

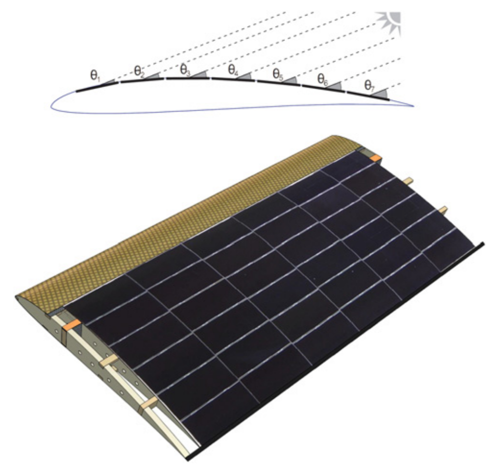


Fig. 13. Variation of incidence angle in cambered arrangement [53].

6. Deviation from tilt angle and geographical location of the flight

Considering the geographical location of the flight, the maximum irradiance and duration of the day in different seasons is not same. Due to low sun elevation in winter, duration of the day and the maximum irradiance decrease. Hence, achieving a continuous flight will be easier in summer. Also to obtain a high endurance flight, the flight orientation should be considered according to the geographical location. Daily solar energy per square meter obtained by a horizontal surface is dependent on geographical location, time, cell orientation and weather conditions and is presented in Eq. (21) (sinusoid model) which can approximate daily solar energy density using maximum irradiance in a day (I_{max}) and duration of the day (T_{day}). In order to take the cloudy days into account, η_{wthr} which is a constant with a value between 1 (clear sky) and 0 (dark) is used in this equation [53].

$$E_{day\ density} = \frac{I_{max} T_{day}}{\pi/2} \quad (21)$$

To keep aerodynamic shape of the wings, the cells be arranged in an arbitrary tilt angle and their arrangement is restricted. So, cells should be arrayed horizontally inside the wing structure or follow the cambered airfoil depending on design, and this results efficiency drop. Furthermore, in a series of cells the one which receives the lowest irradiance limits the current for the others. This problem occurs according to changes in the flight orientation or when the sun elevation is low (sunrise or sunset). As it is shown in Fig. 13, the angle θ_1 has the smallest elevation angle and will penalize the other cells. So to obtain high efficiency, arrangement and keeping the same orientation of the cells should be taken into consideration. Simulations have showed that the cambered shape decreases the obtained energy by almost 10% during a whole day and to take this effect into account, a new efficiency η_{camber} which is above 90% should be considered in Eq.

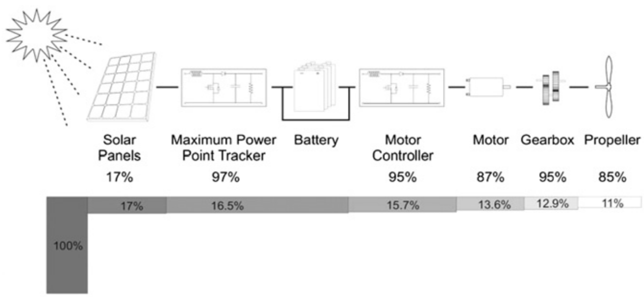


Fig. 14. Energy conversion procedure [32].

(22) to calculate the total produced electric energy from the cells of the wings [53] where η_{mppt} is the efficiency of the maximum power point tracker and A_{sc} is the surface of solar cells in meter.

$$E_{elec\ total} = \frac{I_{max} T_{day}}{\pi/2} A_{sc} \eta_{camber} \eta_{wthr} \eta_{sc} \eta_{mppt} \quad (22)$$

7. Summary and conclusion

To recapitulate, important parameters which influence the output power and efficiency of PV cells should be taken into consideration for achieving desired performance in a solar-powered aircraft. Designing an efficient and lightweight MPPT device to make voltage and current work for a maximum power is a way of reaching to a high endurance flight. Furthermore, type of covering and mounting of the cells affect the received solar radiation, amount of heat transfer on the wings and the output power. Temperature of the cells decreases during the flight and causes increase in efficiency. So this would be a significant factor while designing the aircraft, selecting the cells and covering the wings. Also, this influences the weight, price and the flight duration. Arraying the cells horizontally and not following the optimum tilt angle (because of keeping the airfoil shape of the wings) leads to efficiency degradation. Furthermore, insufficiency of receiving irradiance in one cell due to cambered arrangement results lower received current for the other cells. So arrangement type and considering the cooling effect which make up the negative impacts should be considered in an optimal design. The wind which blows from the opposite side of the flight causes lift force and less power is required for flight in this situation. In addition, wind also decreases temperature of the cells because of convection heat transfer. Hence, considering wind direction and its speed plays an important role in power consumption while selecting flight route and objective definition (especially when flight duration is a major matter). Geographical location and flight orientation are the other discussed factors which influence received radiation and power generation during the flight. As discussed through this paper, a continuous flight is dependent on appropriate designing and selecting efficient devices which lead to less total power loss. Fig. 14 illustrates efficiency of each component and energy conversion procedure for a solar-powered aircraft.

Acknowledgment

The authors would like to thank research center of Islamic Azad University-South Tehran Branch for supporting this research project (Project No. B/16/624).

References

[1] 〈www.nrel.gov〉.
[2] Tiwari GN, Mishra RK, Solanki SC. Photovoltaic modules and their applications: a review on thermal modelling. Applied Energy 2011;88:2287–304.
[3] Tan CM, Chen BKE, Toh KP. Humidity study of a-Si PV cell. Microelectronics Reliability 2010;50:1871–4.
[4] Sugimura RS, Wen LC, Mon GR, Ross RS. Test techniques for voltage/humidity induced degradation of thin-film photovoltaic modules. Solar Cells 1990;28(2): 10314.
[5] Gwandu BAL, Creasey DJ. Humidity: a factor in the appropriate positioning of a photovoltaic power station. Renewable Energy 1995;6(3):3136.
[6] Hottel H, Woertz B. Performance of flat-plate solar-heat collectors. Transactions of the American Society of Mechanical Engineers (USA) 1942:64.
[7] Mani M, Pillai R. Impact of dust on solar photovoltaic (PV) performance: research status, challenges and recommendations. Renewable and Sustainable Energy Reviews 2010;14(9):312431.
[8] Goossens D, Van Kerschaever E. Aeolian dust deposition on photovoltaic solar cells: the effects of wind velocity and airborne dust concentration on cell performance. Solar Energy 1996;66(4):27789.
[9] Sze SM. Physics of semiconductor devices. John Wiley Sons; 1981 p. 264 [chapter 14].
[10] Landis G, Rafaelle R, Merritt D. High temperature solar cell development. In: Proceedings of the 19th European photovoltaic science and engineering conference. Paris, France; 2004.
[11] Wysocki JJ, Rappaport P. Effect of temperature on photovoltaic solar energy conversion. Journal of Applied Physics 1960;31:571578.
[12] Fan JCC. Theoretical temperature dependence of solar cell parameters. Solar Cells 1986;17:309315.
[13] Singh P, Singh SN, Lal M, Husain M. Temperature dependence of IV characteristics and performance parameters of silicon solar cell. Solar Energy Materials and Solar Cells 2008;92:1611161.
[14] Contreras MA, Nakada T, Pudov AO, Sites R. ZnO/ZnS (O,OH)/Cu(In,Ga)Se2/Mo solar cell with 18.6% efficiency. In: Proceedings of the third world conference of photovoltaic energy conversion; 2003. p. 570573.
[15] Friedman DJ. Modeling of tandem cell temperature coefficients. In: Proceedings of the 25th IEEE Photovoltaic Specialists Conference. Washington DC, IEEE, New York; 1996. p. 8992.
[16] Meral ME, Dinçer F. A review of the factors affecting operation and efficiency of photovoltaic based electricity generation systems. Renewable and Sustainable Energy Reviews 2011;15:2176–84.
[17] 〈http://www.pvcdrom.pveducation.org〉.
[18] Singh P, Ravindra NM. Temperature dependence of solar cell performance—an analysis. Solar Energy Materials & Solar Cells 2012;101:36–45.
[19] Smestad GP. Optoelectronics of solar cells. Bellingham, WA: SPIE Press; 2002.
[20] Mattei M, Notton G, Cristofari C, Muselli M, Poggi P. Calculation of the polycrystalline PV module temperature using a simple method of energy balance. Renewable Energy 2006;31:553–67.
[21] Buchet E. du dimensionnement et developpement dun logiciel daide a' la conception de syste'mes de production denergie utilisant la conversion photovoltaique de lenergie solaire. MS thesis: University of Saint Jerome, Marseille, France; 1988.
[22] Messenger RA, Ventre J. Photovoltaic systems engineering. CRC press; 2004.
[23] Sinton R, Cuevas A. Contactless determination of current–voltage characteristics and minority-carrier lifetimes in semiconductors from quasi-steady-state photoconductance data. Applied Physics Letters 1996;69:2510–2.
[24] Skoplaki E, Palyvos J. On the temperature dependence of photovoltaic module electrical performance: a review of efficiency/power correlations. Solar Energy 2009;83(5):61424.
[25] Takun P, Kaitwanidvilai S, Jettanasen C. Maximum power point tracking using fuzzy logic control for photovoltaic systems. In: Proceedings of the international multiconference of engineers and computer scientists (IMESC). Hong Kong, vol. 2; 2011.
[26] Diepeveen N. The Sun-Surfer, Design and construction of a solar powered MAV. Internship Report, Autonomous Systems Lab, ETH Zurich; 2007.
[27] Marshall B. Solar Glider. ENG460, Engineering thesis final report. Murdoch University; 2012.
[28] Matteson A, Leader T, Valentin G, Seagart T, Rodriguez I. Solar jackets maximum power point tracker, Section L01. Georgia Institute of Technology, College of Engineering, School of Electrical and Computer Engineering; 2011.
[29] Sera D. Real-time modelling, diagnostics and optimised MPPT for residential PV systems. Aalborg University; 2009.
[30] Salivahanan S, Kumar N, Vallavaraj A. Electronic devices and circuits. New Delhi: McGraw-Hill; 2008 p. 14.
[31] Mohan N. First course on power electronics. Minneapolis, Minnesota: MNPERE, 2007; 2007.
[32] Noth N, Engel W, Siegwart R. Design of an ultra-lightweight autonomous solar airplane for continuous flight. Autonomous Systems Lab, EPFL. Lausanne, Switzerland; 2006.
[33] Esram T, Chapman PL. Comparison of photovoltaic array maximum power point tracking techniques. IEEE Transactions on Energy Conversion 2007;22 439-7.
[34] Xiao W, Dunford WG. A modified adaptive hill climbing MPPT method for photovoltaic power systems. In: Proceedings of the IEEE 35th annual power electronics specialists conference, PESC 2004;3:1957–63.
[35] Xuesong Z, Daichun S, Youjie M, Deshu C. The simulation and design for MPPT of PV system based on incremental conductance method. In: Proceedings of the WASE International Conference on Information Engineering (ICIE) 2010;2:314–7.

[36] Yusof Y, Sayuti SH, Abdul Latif M, Wanik MZC. Modeling and simulation of maximum power point tracker for photovoltaic system. In: Proceedings of national power and energy conference, PEC 2004:88–93.
[37] Fermia N, Granozio D, Petrone G, Vitelli M. Predictive & adaptive mppt perturb and observe method. IEEE Transactions on Aerospace and Electronic Systems 2007;43:934–50.
[38] Calotes M. Solar power-switching network, solar power array management. Georgia Institute of Technology, Georgia Proposal; September 2010.
[39] Piegari L, Rizzo R. Adaptive perturb and observe algorithm for photovoltaic maximum power point tracking. Renewable Power Generation, IET 2010;4(4): 317–28.
[40] Syafaruddin Karatepe E, Hiyama T. Artificial neural network-polar coordinated fuzzy controller based maximum power point tracking control under partially shaded conditions. Renewable Power Generation, IET 2009;3(2): 239–53.
[41] Subiyanto MA, Hannan MA. Hardware implementation of fuzzy logic based maximum power point tracking controller for PV systems. In: Proceedings of the 4th international power engineering and optimization conference (PEOCO) 2010:435–9.
[42] D'Souza NS, Lopes LAC, Liu X. An intelligent maximum power point tracker using peak current control. In: Proceedings of the IEEE 36th Power Electronics Specialists Conference PESC 2005:172.
[43] Hohm DP, Ropp ME. Comparative study of maximum power point tracking algorithms. Progress in Photovoltaics: Research and Applications 2002;11: 47–61.
[44] Femia N, Petrone G, Spagnuolo G, Vitelli M. Optimizing sampling rate of P&O MPPT technique. In: Proceedings of the Power electronics specialists conference, PESC04 IEEE 35th Annual 2004;3:1945–9.
[45] Brambilla A, Gambarara M, Garutti A, Ronchi F. New approach to photovoltaic arrays maximum power point tracking. In: Proceedings of the Power Electronics Specialists Conference, 1999 PESC 99 30th Annual IEEE 1999;2:632–7.
[46] Sera D, Kerekes T, Teodorescu R, Blaabjerg F. Improved MPPT method for rapidly changing environmental conditions. IEEE ISIE. Montréal, Québec, Canada; 2006.
[47] ON E. Netz—Grid Code. High and Extra High Voltage; 2006.
[48] Noth A. Design of mppt and battery charger. Technical report; 2004.
[49] Myers DR, Emery K, Gueymard C. Revising and validating spectral irradiance reference standards for photovoltaic performance. In: ASES/ASME solar 2002 conference proceeding. Reno, Nevada 2002;1520.
[50] Kurnik J, Jankovec M, Brecl K, Topic M. Outdoor testing of PV module temperature and performance under different mounting and operational conditions. Solar Energy Materials and Solar Cells 2011;95:373–6.
[51] King DL, Boyson WE, Kratochvil JA. Photovoltaic array performance model. Sandia, Sandia National Laboratories, Albuquerque, New Mexico 2004. Report no. SAND2004-3535.
[52] Weider A, Levy H, Regev I, Ankri L, Goldenberg T, Ehrlich Y., et al. SunSailor: solar powered UAV. Technion IIT. Haifa, Israel.
[53] Noth A. Design of solar powered airplanes for continuous flight. Dissertation for the degree of Doctor of Technical Sciences. ETH ZRICH; 2008.
[54] Nusselt W, Jürges W. The cooling of a flat wall by an airstream (Die Kühlung einer ebenen wand durch einen Luftstrom). Gesundh-Ing 1922;52(45):641–2.
[55] Wang X, Bibeau E, Naterer GF. Experimental correlation of forced convection heat transfer from a NACA airfoil. Experimental Thermal and Fluid Science 2007;31:1073–82.